ISEIS

Journal of Environmental Informatics 41(1) 67-74 (2023)

Journal of Environmental Informatics

www.iseis.org/jei

Preparation of Diatomite Based Porous Slow-Release Materials and its Adsorption-Release Properties on Phoxim

Y. Liu[1], Y. Zhang[1], X. R. Sheng[1], N. Li[1], Q. W. Ping[1], M. H. Niu[1], P. Lu[2], and J. Zhang[1, 2 *]

[1] *School of Light Industry and Chemical Engineering, Dalian Polytechnic University, Dalian 116034, China*
[2] *School of Light Industry and Food Engineering, Guangxi University, Nanning 530004, China*

Received 11 Feburary 2021; revised 19 May 2021; accepted 06 July 2021; published online 18 August 2021

ABSTRACT. Slow-release materials have the property of controlling the slow-release of drugs. At present, polymer slow-release materials have been widely studied, but the stability is poor and the release effect of components is difficult to control. The diatomite mineral is light in weight, small in volume and stable in physical and chemical properties. A series of diatomite based porous slow-release materials were prepared to explore the adsorption-release performance. The prepared slow-release materials have excellent porous structure and adsorption-release properties. The adsorption process of phoxim onto slow-release materials accorded with Freundlich model. The maximum adsorption capacity reached 217.86 mg g^{-1} at 25 ºC. In addition, the release effect of phoxim from slow-release materials was obvious under acid or high temperature conditions. The limit release amount was 60.04 and 80.2% respectively. The slow-release time was up to 25 days which will reduce the phoxim residues efficiently. According to the fitting results of Ritger-Peppas model, the release process was controlled by Fick diffusion mechanism.

Keywords: diatomite, adsorption, adsorption isotherm, slow-release, Ritger-Peppas

1. Introduction

Slow-release material is the use of physical or chemical means to store drugs in it, controls the release rate of some active substances in the expected time, maintains a certain effective concentration in a certain system, and slowly releases to the environment in a certain time by means of infiltration, diffusion, precipitation and depolymerization (Yang, 2012; Li et al., 2020).

In recent years, polymers materials (Garrido et al., 2014; Xie et al., 2016) have been usually used as slow-release materials. Although the slow-release materials prepared by natural polymers can improve the slow-release performance, they are easy to degrade and sensitive to the environment, which causes their poor stability and the release of effective components is difficult to control (Amine et al., 2014).

The structure of slow-release material determines its performance, in the process of drug storage, the slow-release materials mainly depend on the adsorption properties of the materials. The slow-release materials with porous structure have the advantages of low relative density, large specific surface area, small specific gravity, high strength, light weight and strong adsorption capacity. Therefore, they are widely applied on the preparation of adsorption type slow-release materials (Chen et al., 1999; Hu et al., 2019).

Diatomite is a kind of natural inorganic clay material which consists of amorphous silica derived from exoskeletons of the single-called diatoms (Tian et al., 2015; Şenol et al., 2019). Diatomite is characterized by unique physical properties, such as high porosity, macro/mesoporous structure, low density, large specific surface area, low cost and nontoxicity (Zhang et al., 2013; Yu et al., 2015). These properties suggest that diatomite is a potential adsorbent (Meng et al., 2013; Ju et al., 2019), fillers (Lamastra et al., 2017; Mold Shukry et al., 2018), catalysis (Cherrak et al., 2016; Son et al., 2016) and drug delivery (Ruggiero et al., 2014; Terracciano et al., 2018). As easily available mineral with excellent properties as mentioned above, diatomite is suitable to prepare slow-release materials.

Phoxim is a typical representative of organophosphorus pesticides, which are common insecticide for pest control. However, the organophosphorus pesticides will seriously endanger human health, especially affect the nervous system. Efficient and safe method to reduce organophosphorus pesticides in agriculture products will contribute to harm reduction and be of environmental interest.

Based on the pervious works on diatomite application, it founded that the diatomite has the excellent adsorption properties on dye, metal ions and antibacterial agent. Furthermore, the physical and chemical modification on diatomite can improve the pore and surface properties efficiently. However, the slow-release properties of diatomite have not been investigated. In

* Corresponding author. Tel.: +86 15942847053.
E-mail address: zhangjian@dlpu.edu.cn (J. Zhang).

ISSN: 1726-2135 print/1684-8799 online
 doi:10.3808/jei.202100468.

this study, a novel porous diatomite based slow-release materials were proposed to realize the slow-release of phoxim and reduce phoxim residues on agriculture products. The absorbing capacity and performance of the slow-release materials were explored by equilibrium and thermodynamics. The mechanism of controlled release of phoxim from slow-release materials was proposed by release kinetics as well. The prepared slow-release materials provided safe and efficient reduction of phoxim in agricultural products.

2. Materials and Methods

2.1. Materials

The diatomite samples were supplied by Jilin Lulin novel materials Co., Ltd., Baishan, Jilin Province, China. Sodium hydroxide, hydrochloric acid, phoxim and methanol were all analytical pure and purchased from Aladdin reagent Co., Ltd.

2.2. Preparation of Slow-Release Materials

The raw diatomite was passed through a 100-mesh metal sieve, and then washed with deionized water. After drying, the selected raw diatomite was used to adsorb phoxim. Then a certain amount of talcum powder and 1% sodium polyacrylate solution were mixed with the diatomite adsorbed phoxim and granulated in powder granulator. The obtained granular material is a kind of slow-release material with raw diatomite, named RDRM. In the same way a kind of slow-release material with calcined diatomite (CDRM) and modified diatomite (MDRM) was prepared respectively. The selected raw diatomite mentioned above diatomite was calcined at 700 ºC for 4 hours to obtain the calcined diatomite. The modified diatomite was obtained by treating the selected raw diatomite with 5% sodium hydroxide at 100 ºC for 2 hours.

The surface area the diatomite materials were determined from the linear part of the BET plot (P/P_0 = 0.05 ~ 0.20) at 77 K using a Quantachrome Autosorb NOVA 2200e volumetric analyzer. Scamming electron microscopy analysis (JEOL, JSM-6460LV) was carried out for the diatomite samples to study the development of morphology and elements. FT-IR spectra of KBr pellets containing the diatomite samples using a Frontier-II series FT-IR spectrometer (PE, USA) in the range from 4,000 cm^{-1} to 400 cm^{-1}.

2.3. Adsorption Studies

The phoxim was used as the adsorbate. The solution of phoxim (100 $mg \cdot L^{-1}$) was prepared with methanol for its bad solubility. Batch adsorption was performed in a set of 50 mL flasks containing 25 mL of phoxim solution with various initial concentrations. The amount of 0.25 g of diatomite and the purified diatomite was added and equilibrated at different temperature in a temperature-controlled water bath shaker (WS-300). After adsorption equilibrium, the concentration of phoxim in the solution was measured using a UV-visible spectrophotometer (PerkinElmer, LAMBDA35) at 280 nm. The adsorption capacity (Q_e) and removal efficiency (E) of phoxim adsorbed onto diatomite were calculated according to the following equations (Yan et al., 2012):

$$Q_e = \frac{(C_0 - C_e)V}{M} \tag{1}$$

$$E(\%) = \frac{(C_0 - C_e) \times 100}{C_0} \tag{2}$$

where Q_e is the adsorption capacity at equilibrium, $mg \cdot g^{-1}$; E is the removal efficiency, %; C_0 and C_e are the initial and equilibrium concentration of phoxim in solution, $mg \cdot L^{-1}$; V is the volume of solution, L; M is the mass of diatomite, g.

The adsorption isotherm was studies using the two well-known isotherm models, Langmuir and Freundlich. The Langmuir model and Freundlich model (Yang et al., 2014) were as follows:

$$\frac{C_e}{Q_e} = \frac{C_e}{Q_{\max}} + \frac{1}{Q_{\max} \cdot K_L} \tag{3}$$

$$\ln Q_e = \ln K_F + \frac{1}{n} \ln C_e \tag{4}$$

where Q_{max} is the maximum adsorption capacity, $mg \cdot g^{-1}$; K_L is a Langmuir constant relate to the affinity of the binding sites and energy of adsorption, $L \cdot g^{-1}$; K_F is a Freundlich constant related to adsorption capacity, $L \cdot g^{-1}$; $1/n$ is an empirical parameter related to adsorption intensity.

The adsorption thermodynamic was carried out in this study to reveal the adsorption properties as well. The thermodynamic parameters for the adsorption process, the standard free energy, standard enthalpy and standard entropy were calculated using the following equations (Chowdhury et al., 2011):

$$\Delta G = -RT \ln K_C \tag{5}$$

$$\Delta G = \Delta H - T\Delta S \tag{6}$$

$$\ln K_C = \frac{\Delta S}{R} - \frac{\Delta H}{RT} \tag{7}$$

where ΔG is the standard free energy, $kJ \cdot mol^{-1}$; R is the universal gas constant, 8.314 $J \cdot mol^{-1} \cdot K^{-1}$; T is the absolute solution temperature, K; ΔH is the standard enthalpy, $kJ \cdot mol^{-1}$; ΔS is the standard entropy, $kJ \cdot mol^{-1} \cdot K^{-1}$. K_c is adsorption equilibrium constant. The standard enthalpy and standard entropy values can be calculated from the slope and intercept of the plot of lnK_c versus $1/T$.

2.4. Release Studies

The modified diatomite slow-release material (1 g) was used to adsorb 6 $mg \cdot mL^{-1}$ phoxim solution at 45 ºC for 3 hours. Talc powder and 1% sodium polyacrylate were added into the slow-release material to obtain phoxim slow-release material.

The effects of temperature and pH on the slow-release properties were studied. A series of 2 g slow-release materials were respectively weighed. After a certain time of reaction, the slow-release material was taken out and the concentration of phoxim in the solution was measured using a UV-visible spectrophotometer (PerkinElmer, LAMBDA35) at 280 nm. The release rate of phoxim onto diatomite was calculated according to the following equation:

$$W = \frac{(1-r_t)100}{R_0} \tag{8}$$

where W is release rate, %; r_t is residual concentration of phoxim at time t, mg·mL^{-1}; R_0 is theoretical release concentration, mg·mL^{-1}.

The slow-release kinetic was studied using the well-known Ritger-Peppas empirical equation. The empirical equation (Lv et al., 2019) is as follows:

$$\frac{M_t}{M_\infty} = Kt^n \tag{9}$$

where M_t / M_∞ is drug cumulative release ratio; t is drug release time, min; K is release rate constant; n is diffusion index.

3. Results and Discussion

3.1. Selection of Slow-Release Materials

Three kinds of slow-release materials of RDRM, CDRM and MDRM were prepared as section 2.2 mentioned above (Figure 1). The adsorption effect of the different slow-release materials was investigated.

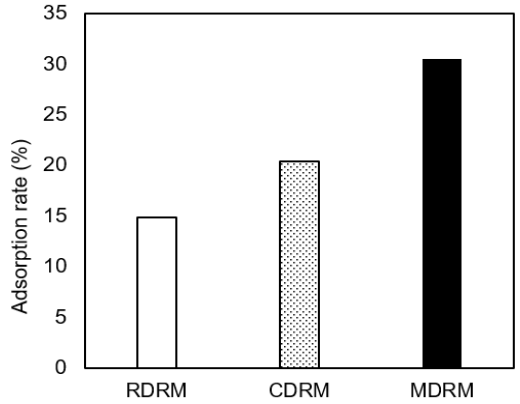

Figure 1. Adsorption effect of different slow-release materials.

By comparing the adsorption rate of three slow-release samples, it indicated that the adsorption capacity of the RDRM was the worst, the CDRM was better and the MDRM was the best. The best adsorption reached 30.43%. The impurities on the surface of diatomite were removed by the treatment of calcination and alkali treatment, which improved the adsorption capacity of the slow-release materials. In addition, some impurities in diatomite pores were cleared by alkali modification deeply which made the adsorption effect of the MDRM better.

3.2. Characteristics of Slow-Release Materials

The quality of slow-release material was directly affected by the adsorption capacity. The characteristics of the different materials were analyzed to optimize the suitable material for adsorbate.

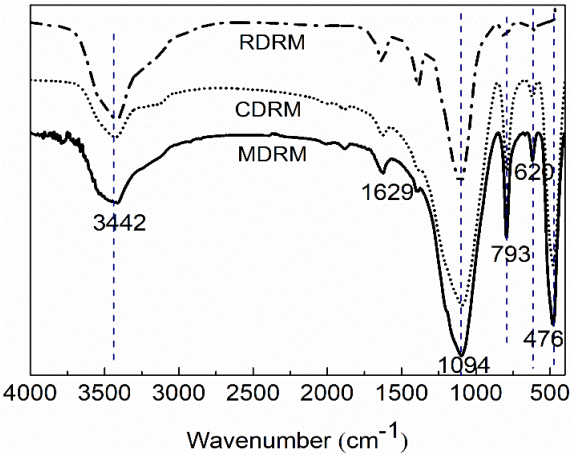

Figure 2. FT-TR spectrogram of diatomite materials.

3.2.1. FI-IR Analysis

The functional groups and chemical bonds of the three slow-release materials were analyzed by infrared spectroscopy and the infrared spectra was shown in Figure 2. The main characteristic peaks of three materials were 476, 620, 793, 1094, 1629, and 3442 cm^{-1} respectively. The peak at 476 cm^{-1} belonged to the Si-O-Si asymmetric stretching modes (Sheng et al., 2009). It can be seen that the peak width of MDRM and CDRM was obviously higher than that of RDRM. The peak at 620 cm^{-1} represented the vibration peak of six membered ring composed of silica tetrahedron in cristobalite which indicated the existence of cristobalite. In the infrared spectrum of the unmodified diatomite, only the vibration absorption peak of Si-O-Si bond was found and there was no 620 cm^{-1} absorption peak which indicated that there was no cristobalite in the unmodified diatomite. The results illuminated that the content of cristobalite in the material increased gradually after high temperature modification (Ren et al., 2016). The peak at 793 cm^{-1} could be determined as Si-OH (Qi et al., 2007). In addition, Si-OH also provided a possibility of chemical adsorption. The peak at 1094 cm^{-1} was considered to be due to Si-O-Si group stretching, and the band at 1629 cm^{-1} was corresponding to H-O-H bending vibration of water (Khraisheh et al., 2005; Caliskan et al., 2011). The peak at 3442 cm^{-1} was due to the vibration absorption peak of Si-OH, the strength decreased with the increase of temperature. Compared with the infrared spectra of the three materials, the infrared spectra of MDRM changed most, especially the peak area of the main functional groups. It indicated that the MDRM had better effect in removing impurities and exposing more pores, which could improve the adsorp-

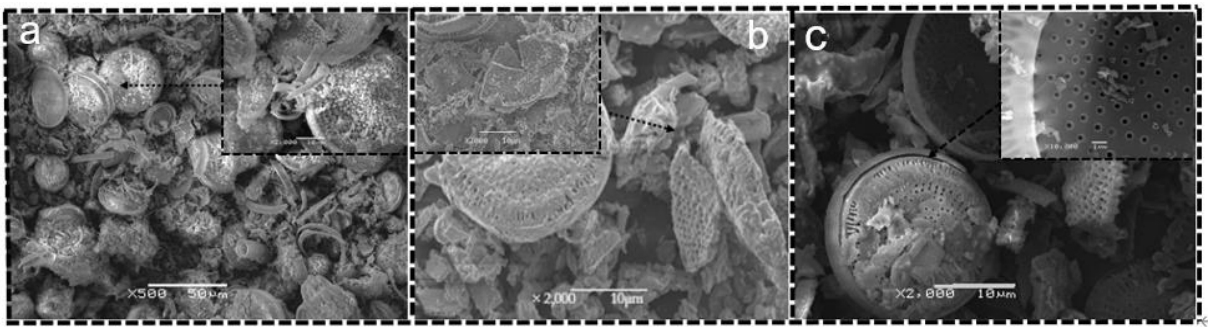

Figure 3. Morphology of RDRM (a), CDRM (b), and MDRM (c).

tion performance of MDRM. It also provided a basis for the preliminary screening of slow-release materials.

3.2.2. SEM Analysis

It can be seen that the prepared slow-release materials were special kind of porous materials (Figure 3). It was a circular sieve plate with a large number of micropores on its surface. The surface morphology of MDRM was better than that of RDRM and CDRM. There were many impurities on the surface of the RDRM, which covered the micropores and blocked the micropores. The impurities in the CDRM samples were slightly less than those of the RDRM. However, the high temperature caused part of the pore structure collapse. After alkali modification, not only the surface impurities of diatomite can be removed, but also the impurities blocking the pores can be cleared, exposing more pore structure which improved the adsorption capability greatly.

3.2.3. BET Analysis

Table 1 showed that the specific surface area and pore size of MDRM were better than that of the RDRM and the CDRM. The impurities removal ability of the alkali modification was better than that of high temperature calcination. In addition, high temperature calcination led to the fragmentation of some diatomite and collapse of some pores, resulting in the smaller specific surface area and pore size. The pore volume of RDRM was the largest, followed by MDRM and CDRM. There were many impurities removed by alkali, while the existence of alkali can react with Si element in diatomite, which led to the disappearance of some fine pore structure and turn into macropores, resulting in the decrease of pore volume. The influence of high temperature calcination made diatomite fragment, collapse, destroyed the pore structure and minimize the pore volume of CDRM. Combined with FT-IR, SEM and BET, the pore structure and properties of MDRM were perfect, which proved the results in Figure 1.

Table 1. BET of Diatomite Samples

	Specific Surface Area $m^2 g^{-1}$	Pore Volume $cm^3 g^{-1}$	Pore Diameter nm
RDRM	20.894	0.2890	5.347
CDRM	22.976	0.0061	5.612
MDRM	34.165	0.0084	6.903

3.3. Adsorption Isotherm

In view of the excellent performance of MDRM, the thermodynamics and kinetics of MDRM were analyzed. Adsorption isotherm was used to describe the effect of different temperature on adsorption, as shown in Figure 4.

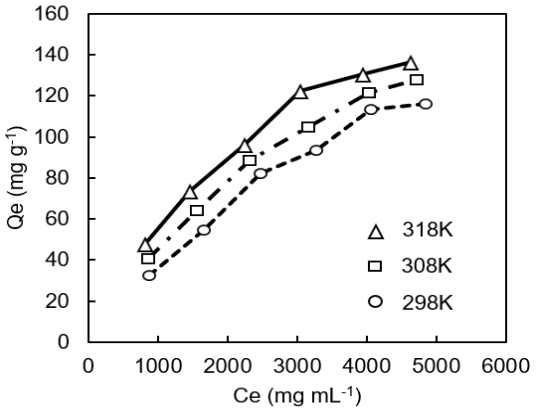

Figure 4. Adsorption isotherm of phoxim onto MDRM.

Figure 4 showed that the adsorption capacity increased with the increase of the concentration of phoxim solution. This may be due to the high molecular content in the solution and the high contact probability with the slow-release material. At the same mass concentration, the increase of temperature increased the adsorption capacity of the slow-release material, it may be caused by the increase of the molecules thermal motion in the solution with the increase of temperature. Phoxim molecules were more likely to contact with the slow-release material in the solution, and more easily adsorbed into the pores of the MDRM. This showed that the appropriate increase of temperature indirectly improved the adsorption capacity of the adsorption material, which was conducive to the adsorption process.

3.4. Adsorption Isotherm Model

The ability of adsorbent to adsorb pollutants in aqueous solution can be described by adsorption isotherm (Sari et al., 2010). In addition, the adsorption of mobile phase on the stationary phase can also be described by adsorption isotherm (Samuelsson et al., 2009). Adsorption isotherm is the relationship between adsorption quantity and concentration of adsor-

Table 2. Adsorption Isotherm Parameters for the Adsorption of Phoxim onto the MDRM

T/ºC	Langmuir			Freundlich		
	Q_{max} / mg g^{-1}	K_L	R^2	K_F	1/*n*	R^2
298K	217.86	0.0002	0.94274	0.2491	0.4543	0.97607
308K	197.23	0.0004	0.97974	0.4190	0.4119	0.99194
318k	190.84	0.0006	0.97696	0.6805	0.3724	0.98184

bent in equilibrium solution at constant temperature, and is the basic requirement of adsorption process design. It is important to obtain parameters from different isotherms for revealing the mechanism of adsorption process and the properties of adsorbents (Zhou et al., 2011). The adsorption of phoxim on diatomite belongs to the adsorption on the solid surface at constant temperature, which is explained by Langmuir and Freundlich isotherm models (Pantoja et al., 2014; Medjdoubi et al., 2019). Langmuir (Foo et al., 2010; Wang et al., 2019) is a monolayer adsorption, the adsorption capacity of each adsorption site is the same and there is no interaction between the adsorbates. Freundlich (Abodif et al., 2020) adsorption isotherm model is multi molecular adsorption, and the surface of adsorbent is not uniform. Langmuir and Freundlich adsorption isotherm models were used to study the effect of phoxim solution with different initial mass concentration at different temperatures, the results were showed in Figures 5 and 6. And the adsorption isotherm parameters of phoxim adsorption onto MDRM samples were listed in Table 2.

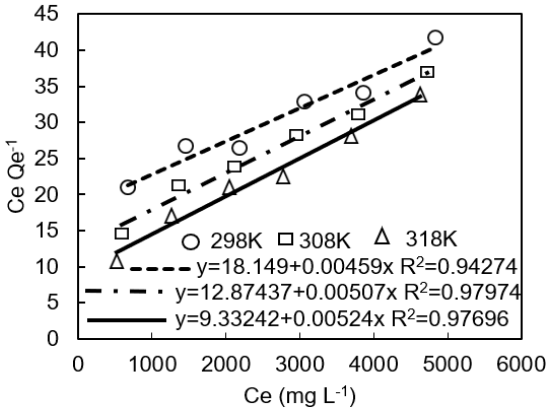

Figure 5. Langmuir isotherm model of phoxim adsorption on MDRM.

It can be seen from Figures 5 and 6 that both Langmuir and Freundlich isotherm equations had good fitting effect, and the fitting effect was also ideal. According to the parameters of Langmuir model, the maximum adsorption capacity of phoxim onto MDRM can reach 217.86 mg·g^{-1} at 25 ºC. However, through the comparison of R^2, the R^2 of Freundlich model was closer to 1, which was more consistent with the hypothesis of sorption theory of phoxim by MDRM. It indicated that chemical adsorption existed in the adsorption process, which was also consistent with the results of FT-IR analysis. In addition, 1/*n* in Table 2 was between 0.5 ~ 1, which indicated that the adsorption of phoxim onto MDRM was monolayer adsorption and the adsorption can be carried out easily. K_L and K_F increased with the increase of temperature. The results showed that temperature affected the adsorption capacity of MDRM. The increase of temperature led to the enhancement of MDRM adsorption capacity. In a word, a proper increase in temperature was effective for adsorption.

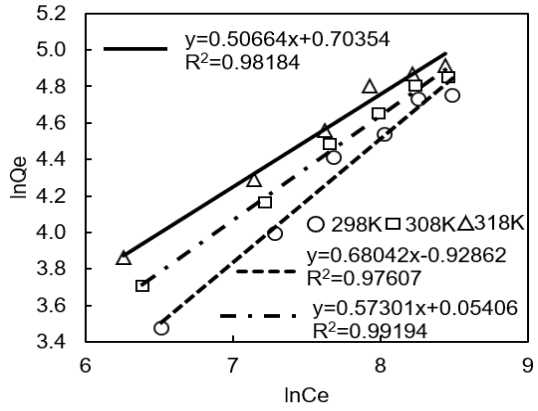

Figure 6. Freundlich isotherm model of phoxim adsorption on MDRM.

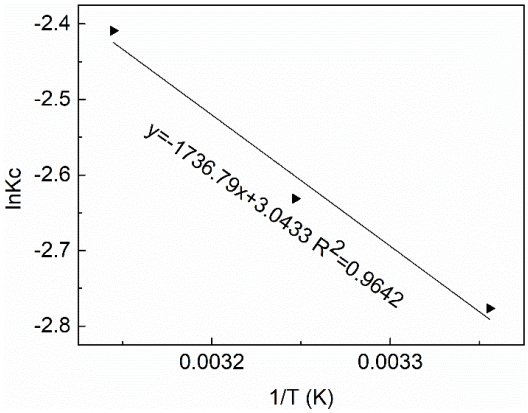

Figure 7. lnK_c-T^{-1} of phoxim adsorption onto MDRM.

3.5. Adsorption Thermodynamics

In order to understand the adsorption process, the thermodynamic parameters were estimated (Table 3). Enthalpy (ΔH) and entropy (ΔS) were obtained from the slope and intercept of K_C versus T^{-1} plot (Figure 7). Gibbs free energy (ΔG) was calculated by Equation (6) (Eltaweil et al., 2020).

It can be seen from Table 3 that ΔS and ΔH were all positive values. The positive value of ΔH indicated that the adsorption process of phoxim onto MDRM was endothermic. The positive ΔS value revealed that the degree of disorder was in-

creased by phoxim onto MDRM (Li et al., 2019). There were both positive and negative values of ΔG, which indicated that when ΔG value was higher than zero at low temperature, it was nonspontaneous reaction. When ΔG value was less than zero at high temperature, it was spontaneous reaction. Therefore, the increase of temperature is conducive to the adsorption process.

Table 3. Thermodynamic Parameters for Phoxim Adsorption onto MDRM

T/K	ΔG/ kJ mol^{-1}	ΔH/kJ mol^{-1}	ΔS/kJ mol^{-1} K^{-1}
298	1.58		
308	0.78	25.51	0.0803
318	−0.02		

3.6 Slow-Release Analysis

3.6.1. pH-Dependence of Slow-Release

Figure 8 showed that on the first day, there was a sudden release phenomenon of slow-release material (pH = 6/7/8). It attributed to the high concentration of phoxim in the slow-release material, which led to the rapid molecular diffusion rate. With the prolongation of the slow-release time, the release rate gradually slowed down and the slow-release amount increased. The slow-release amount of the slow-release material decreased with the increase of pH, the slow-release amount under the acid condition was stronger than that under the alkaline and neutral conditions, but the increase was not very significant.

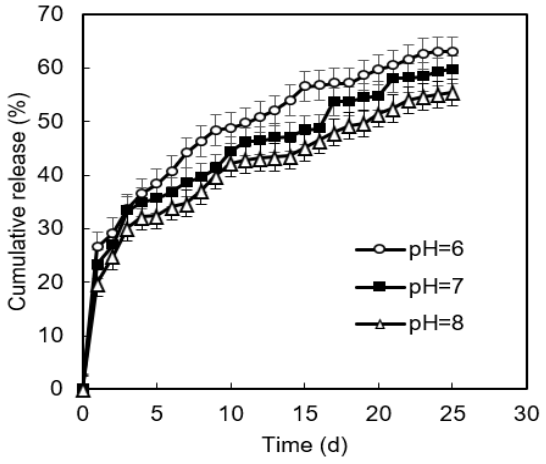

Figure 8. Effect of pH on MDRM.

3.6.2. Temperature-Dependence of Slow-Release

The slow-release amount of the slow-release material also showed a sudden release phenomenon on the first day. With the extension of time, the slow-release amount increased gradually, after four days, the release rate slowed down, but the slow-release amount continued to increase. In addition, the increase of temperature had a good effect on the increase of slow-release amount, especially at 35 ℃, the slow-release effect is more prominent. The sudden release amount on the first day is also high, reached about 30%. More than 80% of the 25 days release amount has been achieved (Figure 9).

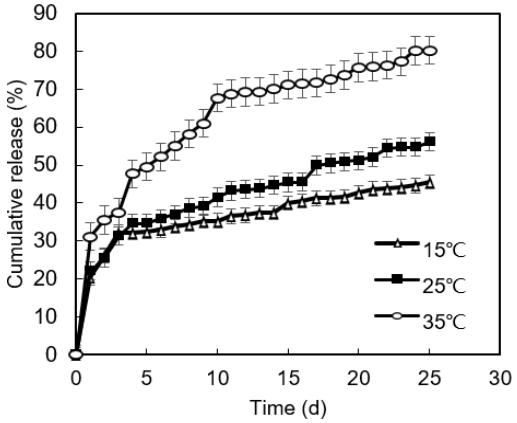

Figure 9. Effect of temperature on phoxim release from MDRM.

3.7 Release Kinetics of Slow-Release Materials

The slow-release is a process of matrix swelling and molecules diffusion from the pores of MDRM. The empirical equation of Ritger-Peppas is used to study the release mechanism.

3.7.1. pH-Dependence of Release Kinetics

Figure 10 showed that according to the Ritger-Peppas release kinetics, the release results of the slow-release materials had good fitting effect. In addition, the fitting data of the model were shown in Table 4.

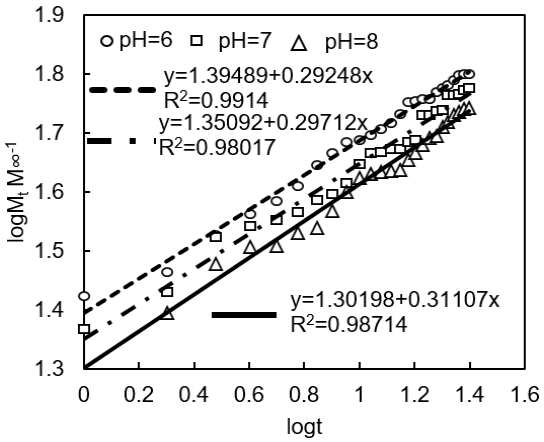

Figure 10. Ritger-Peppas at different pH.

The goodness of fit R^2 were all above 0.98, indicating that the release process was highly fitted to the model. The fitting index n can be used to judge the law of drug release. When $n < 0.5$, it is Fick diffusion; when $0.5 < n < 1.0$, it is abnormal diffusion; when $n > 1.0$, it is class II diffusion. The n value in the table is between 0.2925 ~ 0.3111, less than 0.5, indicating that the slow-release process was controlled by Fick diffusion mechanism under different pH conditions. The K value decreased with the increase of pH, which caused by the decomposition of the phoxim under alkaline conditions and resulting in a certain lower release.

Table 4. Ritger-Peppas Release Model Fitting Results under Different pH Levels

pH	*K*	*n*	R^2
6	24.8256	0.2925	0.9914
7	22.4337	0.2971	0.9802
8	20.0447	0.3111	0.9871

3.7.2. Temperature-Dependence of Release Kinetics

Figure 11 showed that different temperatures had good fitting effect. The cumulative release ratio at 35 ºC was significantly higher than that at 25 and 15 ºC, which was consistent with the release results in Figure 10. The obtained fitting data of the model are listed in Table 5.

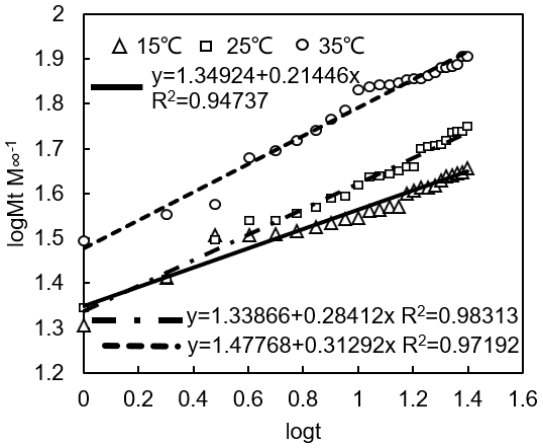

Figure 11. Ritger-Peppas at different temperature.

Table 5. Ritger-Peppas Release Model Fitting Results in Different Temperature

T/ºC	*K*	*n*	R^2
15	22.3460	0.2145	0.9434
25	21.8122	0.2841	0.9831
35	30.0400	0.3129	0.9719

The R^2 was greater than 0.94, indicating that the fitting degree was better. The fitting index *n* is between 0.2145 ~ 0.3126, indicating that phoxim release from slow-release materials was controlled by Fick diffusion mechanism. The *K* value decreased first and then increased with the increase of temperature, which indicated that the release amount of phoxim on the slow-release materials was affected by temperature. The controlled release amount can be achieved by adjusting the temperature properly.

4. Conclusion

Three kinds of slow-release materials (RDRM, CDRM, and MDRM) were prepared from diatomite. It found that the MDRM was the best slow-release material with better morphology structure and higher specific surface area. The adsorption rate reached 30.43%. Based on the study of adsorption thermodynamics and slow-release kinetics, results showed that the adsorption of MDRM was more in line with Freundlich isotherm model and the maximum adsorption capacity reached 217.86 $mg \cdot g^{-1}$ at 25 ºC. The adsorption process had both physical adsorption and chemical adsorption, it belonged to single molecule adsorption. As for the effect of chemical adsorption, it will be discussed in the future work. Slow-release properties at the condition of the acid solution and high temperature can be improved. The slow-release time was up to 25 days. It realized the slow-release of phoxim and reducing the residues in agriculture products effectively. The release law followed Ritger-Peppas equation and the release process was controlled by Fick diffusion mechanism. Through the study of porous diatomite slow-release materials, the theoretical basis for the application of slow-release materials in the future is provided.

In future work, the adsorption-release properties of the slow-release materials based on diatomite will be improved by modified diatomite and prepared process. The mechanism of the slow-release will be further clarified. Efficiency modification of diatomite and preparation of slow-release material are realized by simpler process, which will provide a potential possibility for large-scale industrial production.

Acknowledgements. Authors are grateful to the Opening Project of Guangxi Key Laboratory of Clean Pulp & Papermaking and Pollution Control (No.2019KF20) and Liaoning Provincial Nature Science Fund (No. 2019-ZD-0134).

References

Abodif, A.M., Abodif, A.M., Meng, L., Ma, S., Ahmed, A.S.A., Belvett, N., Wei, Z.Z. and Ning, D. (2020). Mechanisms and models of adsorption: TiO_2-supported biochar for removal of 3,4-dimethylaniline. *ACS Omega*, 5(23), 13630-13640. https://doi.org/10.1021/acsomega.0c00619

Amine, K.M., Champagne, C.P., Raymond, Y., St-Gelais, D., Britten, M., Fustier, P., Salmieri, S. and Lacroix, M. (2014). Survival of microencapsulated Bifidobacterium longum in Cheddar cheese during production and storage. *Food Control*, 37, 193-199. https://doi.org/10.1016/j.foodcont.2013.09.030

Caliskan, N., Kul, A.R., Alkan, S., Sogut, E.G. and Alacabey, I. (2011). Adsorption of Zinc(II) on diatomite and manganese-oxide-modified diatomite: A kinetic and equilibrium study. *J. Hazard. Mater.*, 193, 27-36. https://doi.org/10.1016/j.jhazmat.2011.06.058

Chen, S.Y., Wu, Z.M., Yu, W.B. and Lu, Y.F (1999). Formation, harmfulness, prevention, control and treatment of waters eutrophication. *Environ. Sci. Technol*., (2), 11-15.

Cherrak, R., Hadjel, M., Benderdouche, N., Bellayer, S. and Traisnel, M. (2016). Treatment of recalcitrant organic pollutants in water by heterogeneous catalysis using a mixed material (TiO_2-diatomite of algeria). *Desalin. Water Treat.*, 57(36), 17139-17148. https://doi.org/10.1080/19443994.2016.1162201

Chowdhury, S., Mishra, R., Saha, P. and Kushwaha, P. (2011). Adsorption thermodynamics, kinetics and isosteric heat of adsorption of malachite green onto chemically modified rice husk. *Desalination*, 265(1-3), 159-168. https://doi.org/10.1016/j.desal.2010.07.047

Eltaweil, A.S., Ali Mohamed, H., Abd El-Monaem, E.M. and El-Subruiti, G.M. (2020). Mesoporous magnetic biochar composite for enhanced adsorption of malachite green dye: characterization, adsorption kinetics, thermodynamics and isotherms. *Adv. Powder Technol.*, 31(3), 1253-1263. https://doi.org/10.1016/j.apt.2020.01.005

Foo, K.Y. and Hameed, B.H. (2010). Insights into the modeling of ad-

sorption isotherm systems. *Chem. Eng. J.*, 156(1), 2-10. https://doi.org/10.1016/j.cej.2009.09.013

Garrido, J., Cagide, F., Melle-Franco, M., Borges, F. and Garrido, E.M. (2014). Microencapsulation of herbicide MCPA with native β-cyclodextrin and its methyl and hydroxypropyl derivatives: An experimental and theoretical investigation. *J. Mol. Struct.*, 1061, 76-81. https://doi.org/10.1016/j.molstruc.2013.12.067

Hu, Z.l., Sun, H.X., Wei, H.J., Mou, P. and Li, A. (2019). Research progress of porous materials in the removal of heavy metal ions from wastewater. *New Chem. Mater*., 47 (07), 46-49.

Ju, L., Zhang, P., Huang, Y., Ni, S., Li, J., Qiu, K., Shen, B., Wang, T. and Gao, Q. (2019). Loading of Fe/Al compounds and adsorption of vanadium (V) on diatomite from Changbai Mountain. *Integr. Ferroelectr.*, 197(1), 146-155. https://doi.org/10.1080/10584587.2019. 1592091

Khraisheh, M.A.M., Al-Ghouti, M.A., Allen, S.J. and Ahmad, M.N. (2005). Effect of OH and silanol groups in the removal of dyes from aqueous solution using diatomite. *Water Res.*, 39(5), 922-932. https://doi.org/10.1016/j.watres.2004.12.008

Lamastra, F.R., Mori, S., Cherubini, V., Scarselli, M. and Nanni, F. (2017). A new green methodology for surface modification of diatomite filler in elastomers. *Mater. Chem. Phys.*, 194, 253-160. https://doi.org/10.1016/j.matchemphys.2017.03.050

Li, G.B., Wang, J. and Kong, X.P. (2020). Coprecipitation-based synchronous pesticide encapsulation with chitosan for controlled spinosad release. *Carbohydr. Polym.*, 249, 116865. https://doi.org/10.1016/j.carbpol.2020.116865

Li, Z., Liu, X. and Wang, Y. (2020). Modification of sludge-based biochar and its application to phosphorus adsorption from aqueous solution. *J. Mater. Cycles Waste Manag.*, 22(1), 123-132. https://doi.org/10.1007/s10163-019-00921-6

Lv, J., Sun, B., Jin, J. and Jiang, W. (2019). Mechanical and slow-released property of poly(acrylamide) hydrogel reinforced by diatomite. *Mater. Sci. Eng. C*, 99, 315-321. https://doi.org/10.1016/j.msec.2019.01.109

Medjdoubi, Z., Hachemaoui, M., Boukoussa, B., Hakiki, A., Benguedach, A. and Hamacha, R. (2019). Adsorption behavior of Janus Green B dye on Algerian diatomite. *Mater. Res. Express*, 6(8), 085544. https://doi.org/10.1088/2053-1591/ab2732

Meng, X., Huang, H. and Shi, L. (2013). Reactive mechanism and regeneration performance of NiZnO/Al_2O_3-diatomite adsorbent by reactive adsorption desulfurization. *Ind. Eng. Chem. Res.*, 52(18), 6092-6100. https://doi.org/10.1021/ie303514y

Mohd Shukry, N.A., Abdul Hassan, N., Abdullah, M.E., Hainin, M.R., Yusoff, N.I.M., Mahmud, M.Z.H., Putra Jaya, R., Warid, M.N.M. and Mohd Satar, M.K.I. (2020). Influence of diatomite filler on rheological properties of porous asphalt mastic. *Int. J. Pavement Eng.*, 21(4), 428-436. https://doi.org/10.1080/10298436.2018.1483504

Pantoja, M.L., Jones, H., Garelick, H., Mohamedbakr, H.G. and Burkitbayev, M. (2014). The removal of arsenate from water using iron-modified diatomite (D-Fe): isotherm and column experiments. *Environ. Sci. Pollut. Res.*, 21(1), 495-506. https://doi.org/10.1007/s1135

Qi, X., Liu, M., Chen, Z. and Liang, R. (2007). Preparation and properties of diatomite composite superabsorbent. *Polym. Adv. Technol*, 18(3), 184-193. https://doi.org/10.1002/pat.847

Ren, Z., Gao, H., Guan, J. and Liu, X. (2016). Effects of high temperature modification on structure and filtration properties of diatomite. *Journal Cent. South Univ*. https://doi.org/10.11817/j.issn.1672-7207.2016.07.048

Ruggiero, I., Terracciano, M., Martucci, N.M., De Stefano, L., Migliaccio, N., Tatè, R., Rendina, I., Arcari, P., Lamberti, A. and Rea, I. (2014). Diatomite silica nanoparticles for drug delivery. *Nanoscale Res. Lett.*, 9(1), 1-7. https://doi.org/10.1186/1556-276X-9-329

Samuelsson, J., Arnell, R. and Fornstedt, T. (2009). Potential of adsorption isotherm measurements for closer elucidating of binding in chiral liquid chromatographic phase systems. *J. Sep. Sci.*, 32(10), 1491-1506. https://doi.org/10.1002/jssc.200900165

Sari, A., Çitak, D. and Tuzen, M. (2010). Equilibrium, thermodynamic and kinetic studies on adsorption of Sb(III) from aqueous solution using low-cost natural diatomite. *Chem. Eng. J.*, 162(2), 521-527. https://doi.org/10.1016/j.cej.2010.05.054

Şenol, Z.M., Şenol Arslan, D. and Şimşek, S. (2019). Preparation and characterization of a novel diatomite-based composite and investigation of its adsorption properties for uranyl ions. *J.Radioanal. Nucl. Chem.*, 321(3), 791-803. https://doi.org/10.1007/s10967-019-06662-y

Sheng, G., Wang, S., Hu, J., Lu, Y., Li, J., Dong, Y. and Wang, X. (2009). Adsorption of Pb(II) on diatomite as affected via aqueous solution chemistry and temperature. *Colloids Surfaces A Physico Chem. Eng. Asp.*, 339(1-3), 159-166. https://doi.org/10.1016/j.colsurfa.2009.02.016

Son, B.H.D., Mai, V.Q., Du, D.X., Phong, N.H., Cuong, N.D. and Khieu, D.Q. (2017). Catalytic wet peroxide oxidation of phenol solution over Fe–Mn binary oxides diatomite composite. *J. Porous Mater*, 24(3), 601-611. https://doi.org/10.1007/s10934-016-0296-7

Terracciano, M., De Stefano, L. and Rea, I. (2018). Diatoms green nanotechnology for biosilica-based drug delivery systems. *Pharmaceutics*, 10(4), 242. https://doi.org/10.3390/pharmaceutics10040242

Tian, L., Zhang, J., Shi, H., Li, N. and Ping, Q. (2016). Adsorption of Malachite green by diatomite: equilibrium isotherms and kinetic studies. *J. Dispers. Sci. Technol.*, 37(7), 1059-1066. https://doi.org/10.1080/01932691.2015.1080610

Wang, S., Lee, Y.N., Nam, H., Nam, H. and Kim, H.K. (2019). Chemical activation of porous diatomite ceramic filter for the adsorption of TMA, H_2S, CH_3COOH and NH_3: Isotherm and kinetic studies. *J. Environ. Chem. Eng.*, 7(6), 103481. https://doi.org/10.1016/j.jece.2019.103481

Xie, C.L., Lee, S.S., Choung, S.Y., Kang, S.S. and Choi, Y.J. (2016). Preparation and optimisation of liposome-in-alginate beads containing oyster hydrolysate for sustained release. *Int. J. Food Sci. Technol.*, 51(10), 2209-2216. https://doi.org/10.1111/ijfs.13207

Yan, B., Zhou, J.T., Li, Y.G., Shi, Q., Fu, H.Y., Chai, T. and Liu, J.F. (2012). Characteristics and thermodynamics of biosorption copper by a newly isolated Penicillium sp. QQ using a response surface methodology. *J. Environ. Informatics*, 19(1). https://doi.org/10.3808/jei.201200208

Yang, J., Yu, M. and Qiu, T. (2014). Adsorption thermodynamics and kinetics of Cr (VI) on KIP210 resin. *J. Ind. Eng. Chem.*, 20(2), 480-486. https://doi.org/10.1016/j.jiec.2013.05.005

Yang, S.Z. (2012). Research progress of pesticide sustained release agent. *Shanxi Agric. Sci*., 40 (02), 186-188. https://doi.org/10.3969/j.issn.10 02-2481.2012.02.26.

Yu, W., Deng, L., Yuan, P., Liu, D., Yuan, W., Liu, P., He, H., Li, Z. and Chen, F. (2015). Surface silylation of natural mesoporous/macroporous diatomite for adsorption of benzene. *J. Colloid Interface Sci.*, 448, 545-552. https://doi.org/10.1016/j.jcis.2015.02.067

Zhang, J., Ping, Q., Niu, M., Shi, H. and Li, N. (2013). Kinetics and equilibrium studies from the methylene blue adsorption on diatomite treated with sodium hydroxide. *Appl. Clay Sci.*, 83, 12-16. https://doi.org/10.1016/j.clay.2013.08.008

Zhou, X., Fan, J., Li, N., Qian, W., Lin, X., Wu, J., Xiong, J., Bai, J. and Ying, H. (2011). Adsorption thermodynamics and kinetics of uridine 5′-monophosphate on a gel-type anion exchange resin. *Ind. Eng. Chem. Res.*, 50(15), 9270-9279. https://doi.org/10.1021/ie101721a